Solid Freeform Fabrication 2025: Proceedings of the 36th Annual International Solid Freeform Fabrication Symposium – An Additive Manufacturing Conference
Reviewed Paper

Pulsed Robotic Wire Arc Additive Manufacturing of 316 L Stainless Steel for Forging Preforms

Stibitz Christin[1], Stevens Hill[1], Jared Seals[1], Hossein Taheri[2] and Bishal Silwal[1]

1 Mechanical Engineering Department, Georgia Southern University

2 Manufacturing Engineering Department, Georgia Southern University

Abstract:

This study explores the use of Robotic Wire Arc Additive Manufacturing (WAAM) to fabricate large-scale 316L stainless steel structures for potential forging preforms. A full wall sample was successfully printed using a robotic WAAM setup equipped with a pulsed Gas Metal Arc Welding (GMAW) process. To investigate the thermomechanical properties of the printed material, compression tests were conducted at a preheat temperature of 1600 °F (871 °C) and a strain rate of 0.01 (in/in)s^{-1}. A custom-designed nickel-based alloy platen was fabricated to perform the high-temperature tests. The data were recorded during testing and flow stress were calculated for the samples. The results demonstrate that WAAM can produce 316L stainless steel components with favorable thermomechanical properties such as hardness and flow stress values between WAAM stainless 316L and extruded stainless 316L samples. These results under forging-like conditions suggest their potential as a cost-effective alternative for manufacturing preforms in forging industries.

Introduction:

Metal 3D printing has potential as a promising alternative to traditional metal forming processes such as casting and forging. Preform forging is a process where a roughly shaped initial workpiece, called a preform, is first made to closely resemble the final part before the final forging operation. This Preform forging reduces the number of forging steps, material waste, and tooling costs. Selective Laser Melting (SLM) has been investigated for creating these preforms with complex geometries that would be difficult or costly to achieve with traditional methods. The study by Sizova et al. [1], shows that titanium alloy parts produced by SLM not only allow for near-net shape production but also demonstrate better hot workability using heat treatment and hot compression testing. Their result reveals SLM parts with lower activation energy and allows faster microstructural refinement which in turn enables easier hot deformation and faster dynamic recrystallization. This also improves forgeability compared to conventionally cast or forged materials. Such combination of additive manufacturing and forging can streamline production, reduce costs, and improve material properties. In this study by Schmidt and Spieth [2], the solid base body of the component is initially forged near-net shape and mechanically machined to prepare precise joining surfaces. Subsequently, selective laser melting (SLM) is employed to build the complex geometries directly onto the forged base, taking advantage of the design flexibility inherent in additive manufacturing. In the study by Fousová [3], various metal 3D printing techniques—including Selective Laser Sintering (SLS), Direct Metal Laser Sintering (DMLS), Electron Beam Melting (EBM), and Selective Laser Melting (SLM)—are reviewed as potential substitutes for conventional manufacturing methods. These additive manufacturing (AM) approaches enable the fabrication of highly complex geometries, minimize material waste, and allow for customization, especially in fields such as medical implants and aerospace components. In this study WAAM was chosen due to its higher deposition rate, lower cost, and ability to fabricate large preforms, which are more relevant for forging industries than the complex geometries enabled by SLM.

Wire arc additive manufacturing (WAAM) is gaining increasing importance due to its unique combination of economic, technical, and practical advantages, especially for large-scale metal part production. WAAM has potential to fabricate medium to large scale preform for forging application at a higher deposition rate compare to SLM. The goal of this research is to investigate the Robotic WAAM to fabricate stainless steel preform in forgings. In Wire Arc Additive Manufacturing (WAAM), the type of power source used depends on the arc welding process selected Gas Metal Arc Welding (GMAW), Gas Tungsten Arc Welding (GTAW), or Plasma Arc Welding (PAW). Researchers have put significant amounts of effort into fabricating stainless-steel parts using WAAM, especially 316 L stainless steel. Cold metal transfer (CMT), a subset of GMAW process known for its adaptive arc control, precision and low heat input, has been utilized the most [4], [5], [6], [7], [8]. The cold metal transfer ensures stable arc behavior and minimal spatter, which is critical in achieving high-quality builds with low surface roughness and minimal defects. While many works are performed using CMT, very few works are published using other GMAW processes. Vishnukumar et al. [9], explored the fabrication of SS316L stainless steel components using Gas Metal Arc Welding (GMAW) in a WAAM setup, emphasizing the influence of post-heat treatment on mechanical and corrosion behavior of 316L stainless steel. In the study conducted by Duan and Yang [10], an innovative approach to (WAAM) was adopted, known as Pulsed Arc Plasma Wire Arc Additive Manufacturing (PAP-WAAM). This technique was developed to overcome the limitations associated with conventional WAAM, particularly the excessive heat input that typically results in coarse microstructures and diminished mechanical properties. The key innovation in PAP-WAAM lies in the pulsed mode application of the arc plasma. Unlike traditional constant-current systems used in Gas Tungsten Wire Arc Additive Manufacturing (GT-WAAM), PAP-WAAM utilizes a pulsed discharge arc, which alternates between ignition and extinguishment cycles.

The objective of this research is to conduct the compression test and analyze the thermomechanical properties, mainly flow stress-strain of the WAAM printed 316L stainless steel at a temperature of 1600 °F (871 °C) and strain rate of 0.01 (in/in)s^{-1}. We are using

Pulsed GMAW, which was selected for its lower heat input and more stable arc compared to conventional GMAW, as supported by Duan & Yang [10]. A compression platen that can withstand a temperature of 300 °C was also designed and fabricated to conduct the test.

Experimental Methods:

A Robotic WAAM setup that consists of Kuka KR-6 controller and Lincoln Electric R450 welder was used to fabricate approximate 0.75 x 11.00 x 6.00 inch wall as shown in Fig 1. A GMAW pulse mode Ultimarc waveform was used. The shielding gas mixture of Ar+CO_2+O_2 was used with a flow rate of 16.5 L/min. The experiment was conducted with a voltage of 28.65 V and current 375 A. The wire feed speed was maintained at 158.75 mm/s and the robot travel speed of 12.7 mm/s.

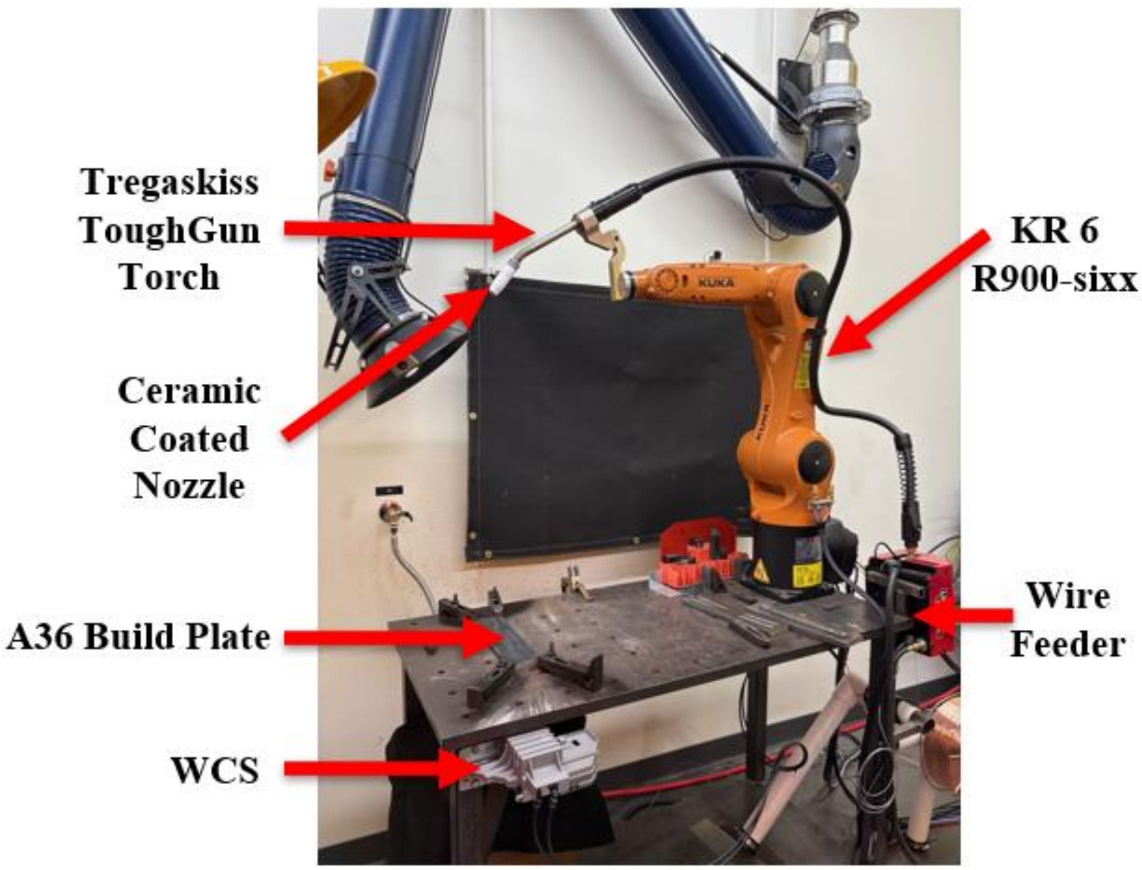

Figure 1. Robotic WAAM setup

Once the wall sample has been successfully printed, the compression test specimens - cylindrical samples of 12.7 mm diameter × 19 mm height were wire-cut from the WAAM wall (ASTM E9 dimensions) as illustrated in Fig 2. Compression tests were conducted on selected randomly selected samples-specifically, 1E, 1K, 2D, 2E, and 2L so that we get the various wall regions to capture representative material variability.

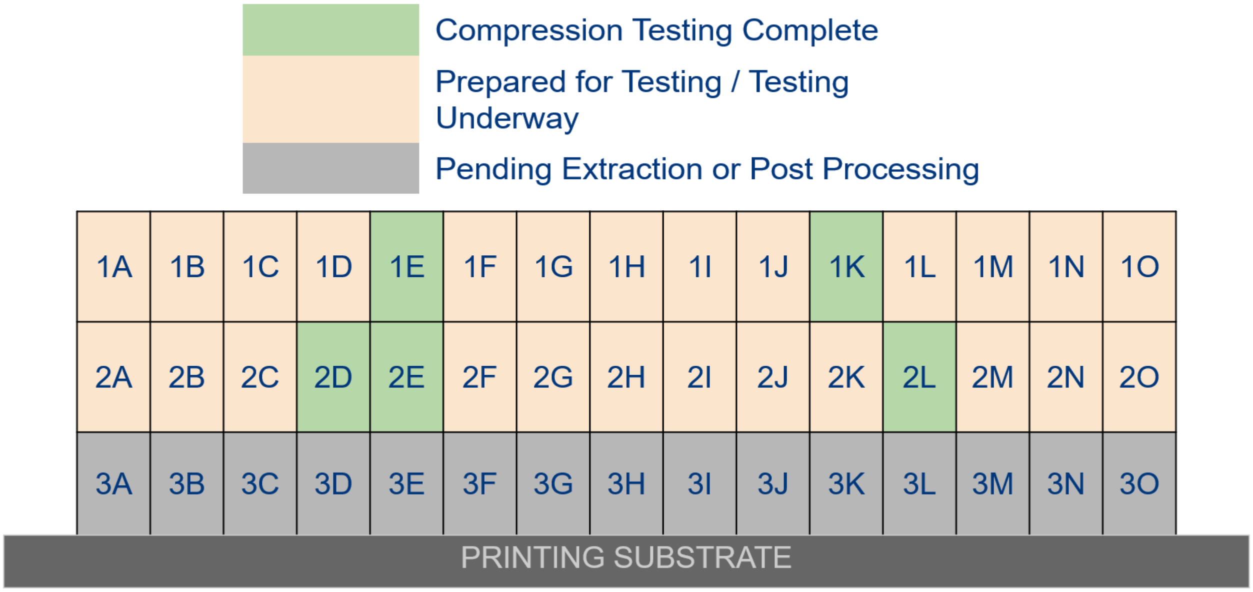

Figure 2. Selection of compression testing specimen from the WAAM printed wall

To evaluate the compressive mechanical behavior of the WAAM printed samples under elevated temperature conditions, and to replicate the industry forging process, a high-temperature compression testing protocol was employed. Prior to heating, each sample was positioned between the compression platens of the testing machine to establish a reference alignment as shown in Fig 3. A home position was defined near the surface of the sample to ensure consistent initial contact during the testing phase. Once the reference setup was complete, the top platen was removed.

Figure 3. A flat compression platen with recession in the middle

The samples were transferred into a high-temperature oven preheated to 1600 °F (871 °C). Heating continued until the samples began to illustrate a visible red-orange glow, indicating that the desired thermal condition had been reached. To ensure thermal equilibrium throughout the sample volume, the specimens were soaked in the oven at this temperature for an additional 15 minutes. Fig 4. shows the 250 kN Hydraulic stand and the high temperature oven used for compression testing.

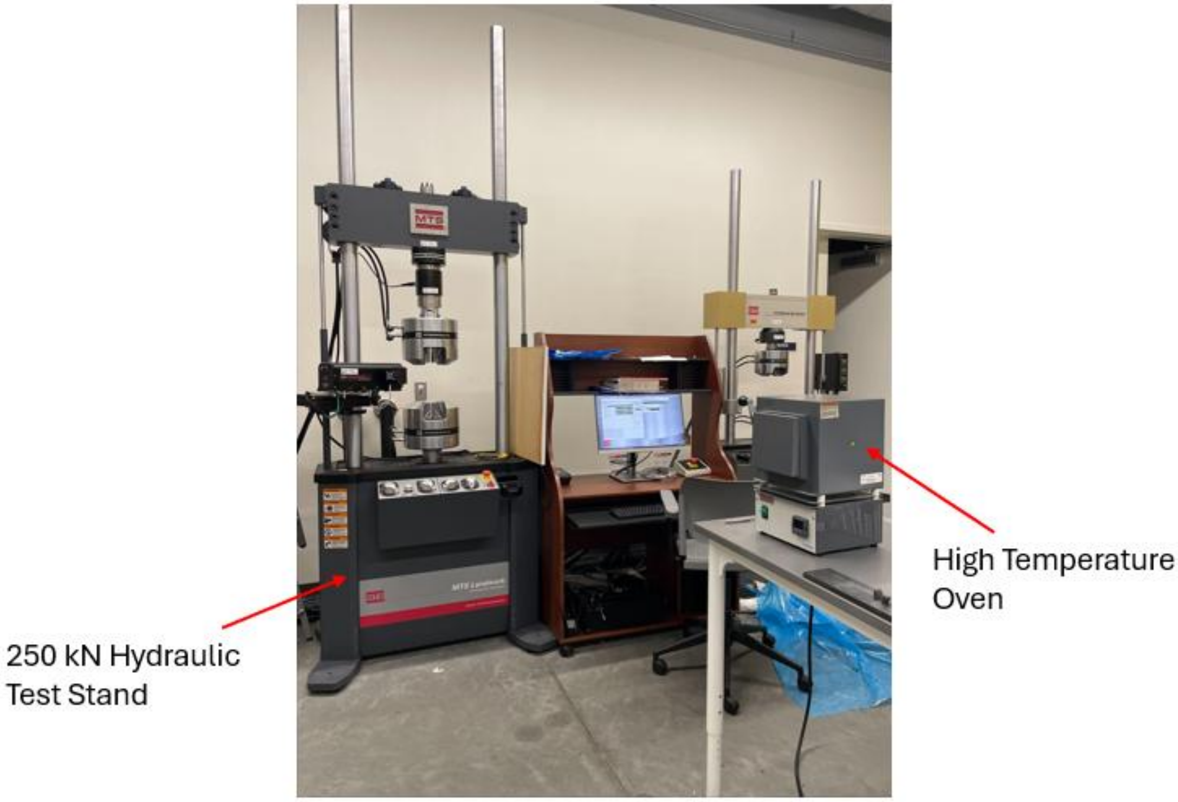

Figure 4. Compression Test Equipment and Oven

After heating, the samples were immediately placed in the platen and once proper alignment and positioning were confirmed, compression testing commenced under controlled loading conditions as shown in Fig 5. All tests were performed under displacement control at a constant strain rate of 0.01 (in/in)s^{-1}. The test setup was constrained by a maximum allowable load of 150 kN, with the exception of the initial test (Sample 1K), which was limited to 100 kN to prevent premature failure. The system also imposed a maximum allowable deflection of 10.16 mm to ensure mechanical integrity and equipment safety during high-temperature operation.

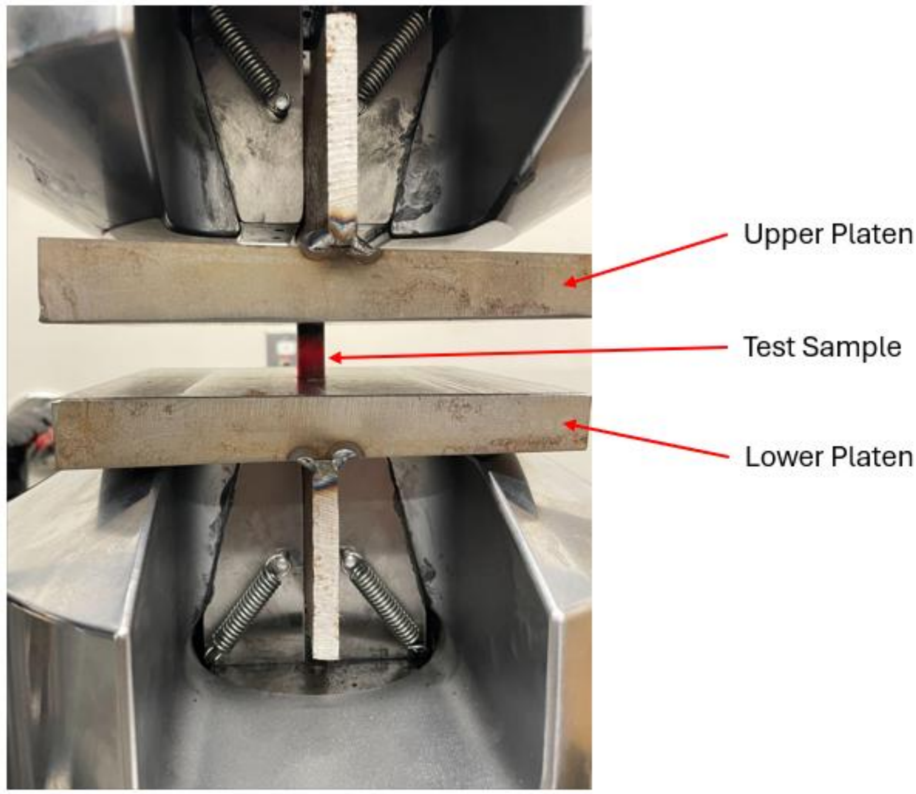

Figure 5. Compression Testing at 1600 °F (871 °C).

Results and Discussion:

The specimens before and after the compression tests are as shown in Fig 6. The specimens experienced barreling due to friction between the platen and the specimens.

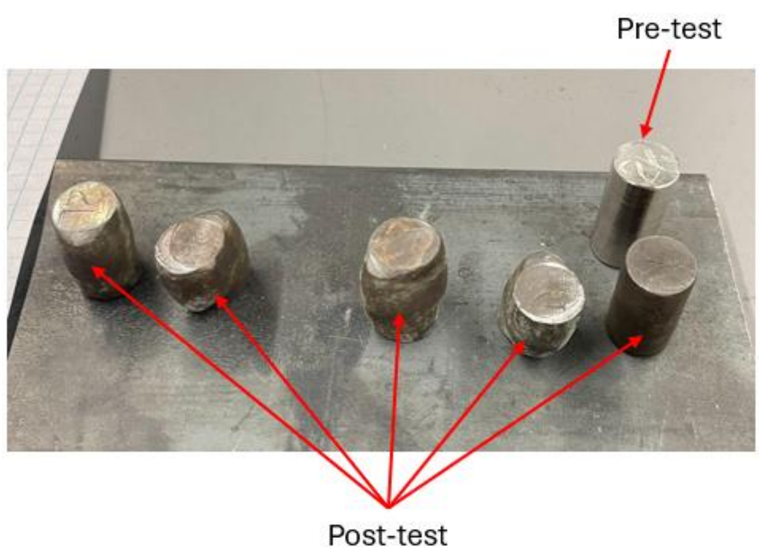

Figure 6. Pre-test and Post-test samples.

Throughout the test, real-time data for temperature, axial load, and deformation were continuously recorded. Using the recorded values of displacement and load, the engineering stress, engineering strain, true stress, and true strain were calculated using the below formulas. Barrelling and bulging of the specimen were observed during the test (Fig 6), primarily due to friction between the platen and the workpiece. However, this deformation was not considered in the subsequent stress–strain analysis. The current equation used provides the flow stress for the uniform deformation.

Engineering Stress (σ_e):

$$\sigma_e = F/A$$

where:

- *F = applied load*
- *A_0 = original cross-sectional area*

Engineering Strain (ε_e):

$$\varepsilon_e = \Delta L/L_0$$

where:

- *ΔL = change in length*
- *L_0 = original length*

True stress = engineering stress × (1 + engineering strain)

True strain = ln (1 + engineering strain)

This enabled detailed analysis of the stress-strain response and the evaluation of temperature-dependent deformation behavior of the WAAM-processed 316L stainless steel. The engineering stress-strain curves for the cold compression platen verification tests are shown in Fig 7. Among the cold-tested samples, Sample 2D exhibited the highest peak stress, reaching around 1177 MPa. Samples 2L, 2E, and 1E followed with peak stresses of approximately 1069 MPa, 1043 MPa, and 1058 MPa, respectively. These results are due to work hardening of the samples.

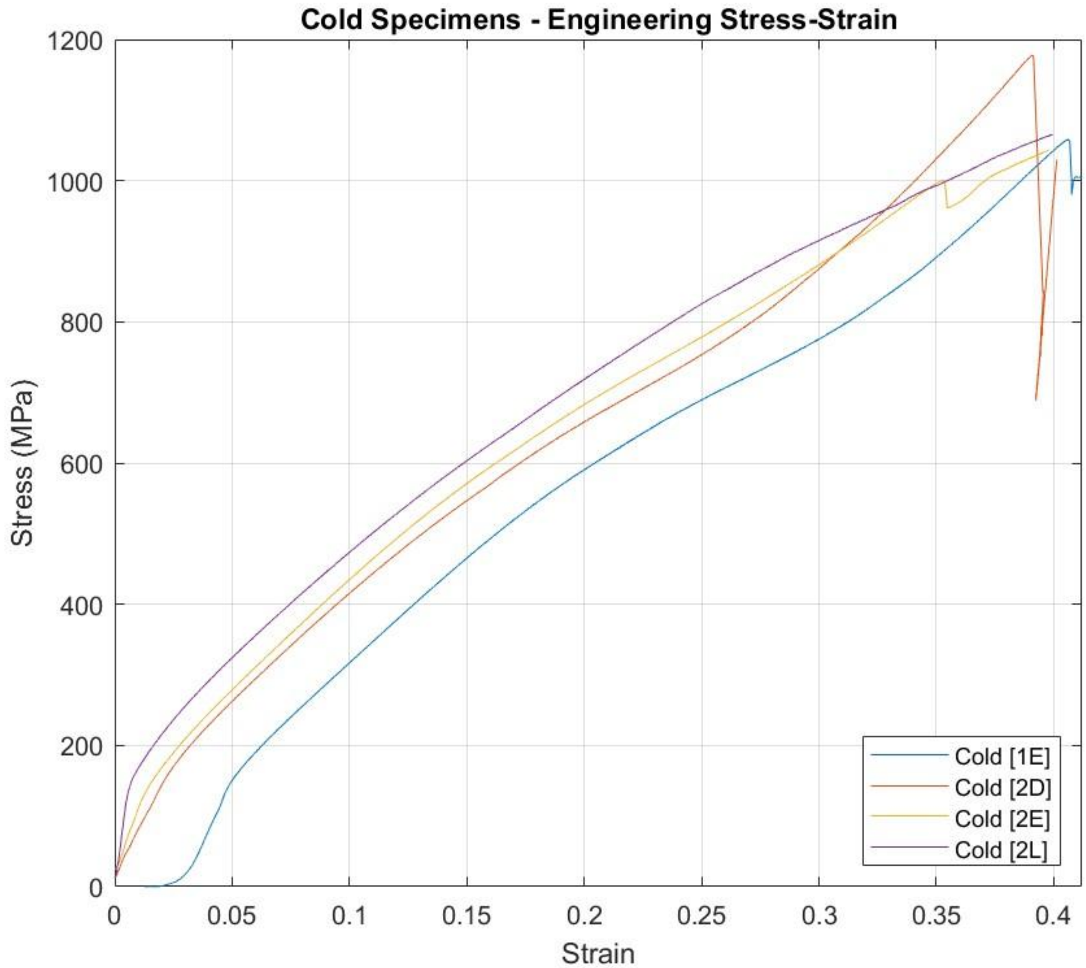

Figure 7. Engineering stress versus Engineering Strain Plot for cold platens

The true stress-strain behavior for the cold compression platen tests is shown in Fig 8. In the cold tests, Sample 2D reached the highest true stress of around 700 MPa, followed by Samples 2L, 2E, and 1E, which all achieved peak stresses between approximately 600 and 650 MPa. Among the tested cold specimens, all curves except for 2D shows strain hardening (based on flow curve) throughout deformation, whereas specimen 2D shows dynamic recovery, as indicated by the reduced hardening rate at higher strains. This may be due to several reason such as temperature drop due to cold platen in contact with the hot samples and the slower strain rate.

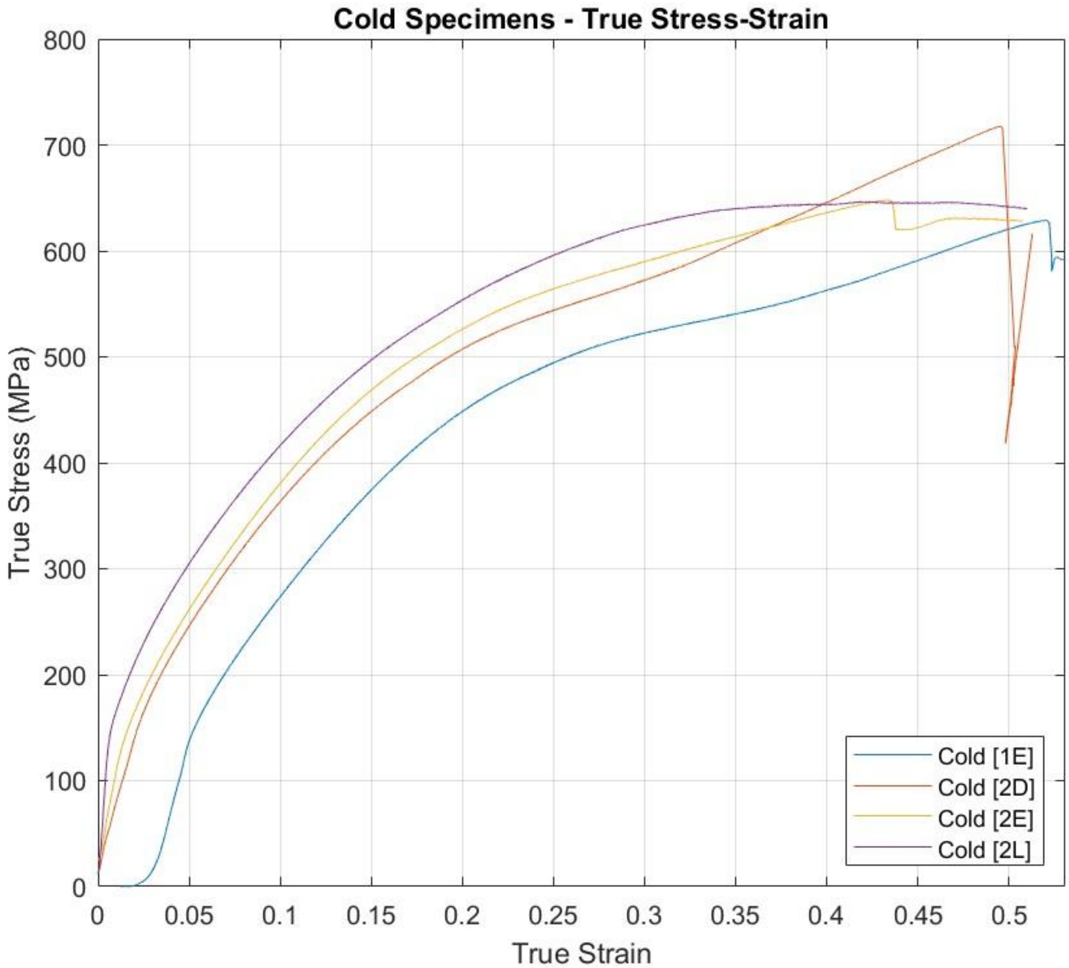

Figure 8. True stress versus True Strain Plot for cold platens

Compression tests were carried out for WAAM printed walls and extruded stainless steel 316 L rod at room temperature and 1600 °F (871 °C) pre-heat for verification purposes. It should be noted that there might have been some temperature drop during specimen heat-transfer to the platens, which was not accounted for in the analysis. The plots for engineering stress vs engineering strain are shown in Fig 9 and 10. On comparison it shows that WAAM samples require less force to deform when compared to a regular extruded 316 L sample, which is favorable for making WAAM produced parts for forging.

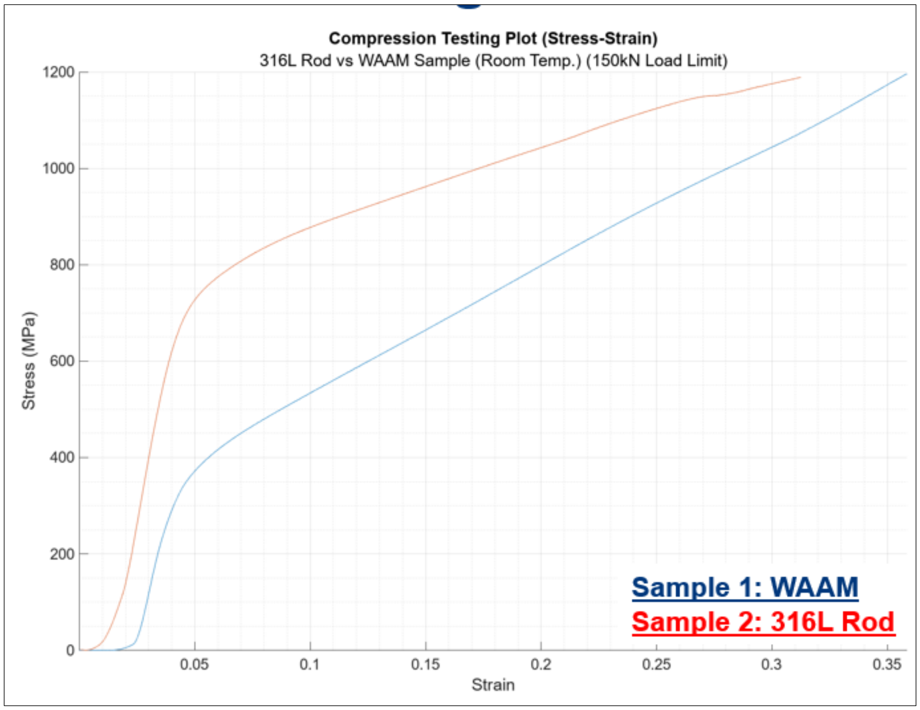

Figure 9. Compression test plot of Engineering stress vs Engineering strain at room temperature.

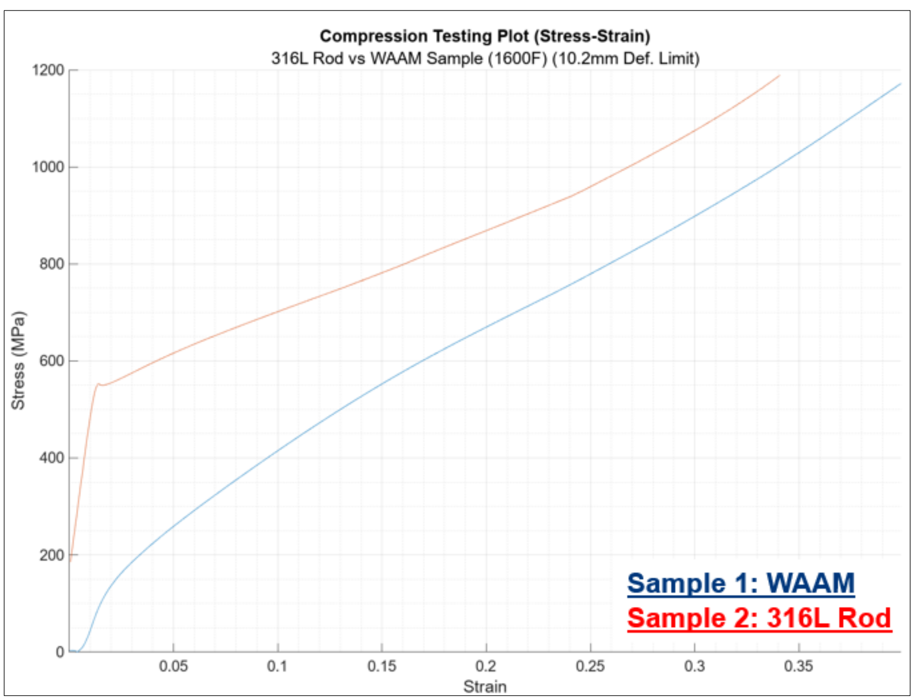

Figure 10. Compression test plot of Engineering stress vs Engineering strain at 1600°F.

To overcome the shortcoming of the current platen and to reduce the temperature difference between the platen surface and heated test specimen, a new platen was designed and fabricated using a nickel-based alloy (Inconel 718). The platen was designed to withstand the repeated compression testing at loads up to 150 kN, for which ½” sample diameter was considered. It also had to withstand preheat temperatures of 300 °C so factors such as oxidation, thermal cracking creep and loss of strength at temperature were taken into account. In addition to this, the platen was designed to include temperature control and heating system for which the following factors were considered. It must be capable of heating platens using a typical single-phase 20A wall outlet. It must independently control the temperatures as heat migration will result in different heating requirements for top and bottom platens. The system must also be ensured safe electrically and thermally for testing purpose.

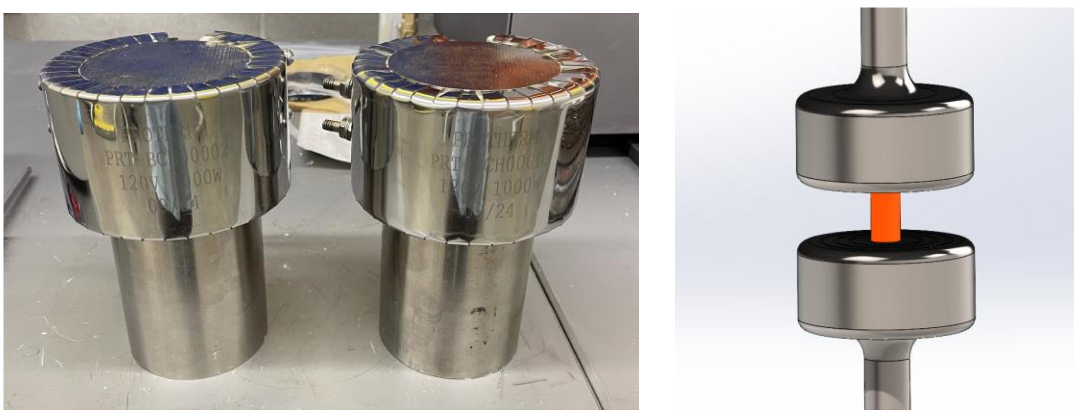

Figure 11. Platen before machining (left) and designed Platen and compression sample (right)

A nickel-based superalloy was selected as a platen material. As per the literature, the yield stress (σ_{yield}) is 1096 MPa and Modulus of Elasticity (E) is 184 GPa at the temperature 600 °F (300 °C). Using these values the allowable force by Shank diameter and Sample diameter were calculated as follows:

- Allowable Force By Shank Diameter (0.770”)

  $A_c = 0.465\ in^2 = 0.0003\ m^2$

  $F_{allow} = \sigma_{yield} * A_c = (1096\ MPa) * (0.0003\ m^2)$

  $F_{allow} = 328.8\ kN >> 150\ kN$ Test Load

- Allowable Force By Sample Diameter (0.5”)

  $A_c = 0.196\ in^2 = 0.00013\ m^2$

$F_{allow} = \sigma_{yield} * A_c = (1096\ MPa) * (0.00013\ m^2)$

$F_{allow} = 142.5\ kN$ ~~< 150 kN Test Load

Some plastic deformation may be seen at the point where sample loading occurs depending upon surface hardness and the number of cycles performed while testing.

Further, the platens were subjected to heat treatment as per AMS 5662 specification for Inconel 718 in an inert atmosphere to age for 8 hours at temperature 1325 - 1400° F (718 - 760° C). Then the furnace was cooled at 100° F (38° C) per hour to achieve 1150 - 1200° F (621 - 649° C). The platen was kept it for 8 hours and then air cooled. The top of the platens surface was grounded to ensure flatness following possible distortion during heat treatment. A band heater (Fig 12) was used to wrap around the circumference of the platen and a PID controller was used to heat the band heater and maintain a constant temperature of 300 °C.

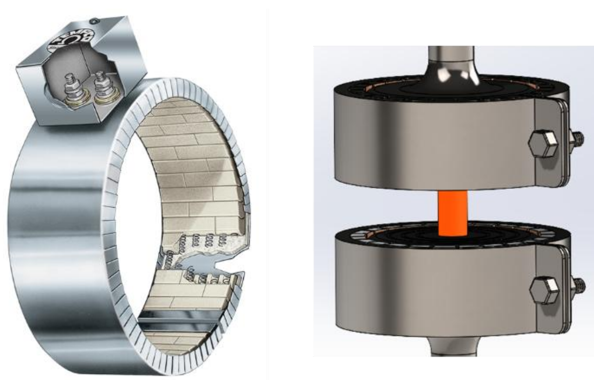

Figure 12. Band heaters used to heat the platens.

After the successful fabrication of preheated platen, the compression test was performed at the strain rate of 0.01 $(in/in)s^{-1}$ and the specimen pre-heat temperature of 1600 °F (871 °C). The results were plotted for Engineering stress vs Engineering strain and true stress vs true strain as shown in Fig 13.

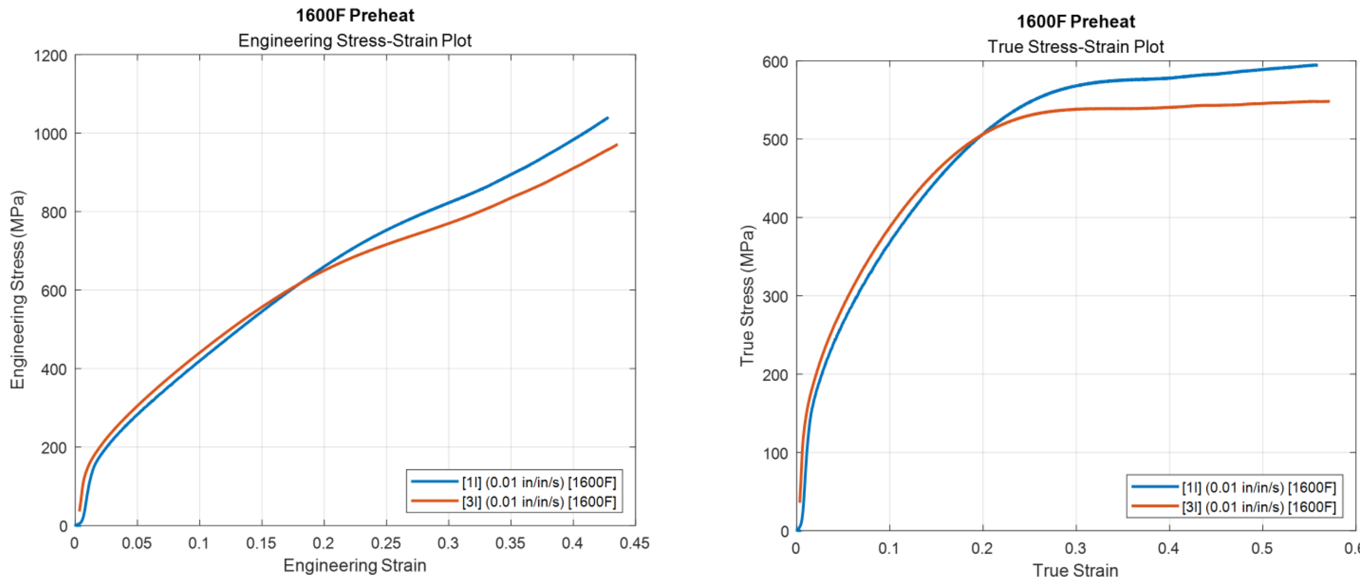

Figure 13. Stress - Strain Plot for samples 1I and 3I with heated platen

The samples tested with the cold platen and hot platen all showed flow stress values between 500 to 600 MPa, with some sample showing higher than 600 MPa when using the cold platen. This change in flow stress at elevated temperatures is mainly due to thermal softening of the material and due to higher temperature difference between the platen surface and tested specimen, which reduces its ability to resist deformation.

Conclusion

1. Robotic Wire Arc Additive Manufacturing (WAAM) was successfully employed to fabricate a structure of 0.75 x 11.00 x 6.00-inch wall using 316 L stainless steel. This demonstrates the capability of WAAM to produce large-scale metal components with potential applications in preform forging.

2. Compression test at room temperature of the WAAM printed sample show lower stress than the extruded 316 L sample. At room temperature, WAAM's lower strength may be due to the anisotropic microstructure compared to the recrystallized grain structure typically observed on the extruded samples.

3. A specialized preheated compression platen as well as the control system was designed and fabricated, capable of operating at elevated temperatures and high loads.

4. Compression tests were conducted at a preheat temperature of 1600 °F (871 °C) and a constant strain rate of 0.01 (in/in)s^{-1}using both the cold and hot platen. The test results showed that using hot platen is more effective in lowering the temperature difference between the platen and sample allowing to achieve the lower flow stress values.

Acknowledgment: This material is based on research sponsored by Air Force Research Laboratory under Agreement Number FA8650-20-2-5700. The U.S. Government is authorized to reproduce and distribute reprints for Governmental purposes not withstanding any copyright notation thereon.

REFERENCES

[1] I. Sizova and M. Bambach, "Hot workability and microstructure evolution of pre-forms for forgings produced by additive manufacturing," *J Mater Process Technol*, vol. 256, pp. 154–159, Jun. 2018, doi: 10.1016/J.JMATPROTEC.2018.02.017.

[2] H. and H. C. and K. C. Schmidt Mario and Spieth, "Hybrid component manufacturing – combining forging and metal 3D printing," in *100 Pioneers in Efficient Resource Management: Best practice cases from producing companies*, Berlin, Heidelberg: Springer Berlin Heidelberg, 2019, pp. 306–309. doi: 10.1007/978-3-662-56745-6_61.

[3] M. Fousová, D. Vojtěch, J. Kubásek, D. Dvorský, and M. Machová, "3D Printing as an Alternative to Casting, Forging and Machining Technologies?," *Manufacturing Technology*, vol. 15, no. 5, pp. 17–18, 2015, doi: 10.21062/UJEP/X.2015/A/1213-2489/MT/15/5/809.

[4] D. G. Andrade, T. Tankova, C. Zhu, R. Branco, L. S. da Silva, and D. M. Rodrigues, "Mechanical properties of 3D printed CMT-WAAM 316 LSi stainless steel walls," *J Constr Steel Res*, vol. 215, p. 108527, Apr. 2024, doi: 10.1016/J.JCSR.2024.108527.

[5] W. Zuo *et al.*, "Experimental investigation on double-lap shear behavior of 3D printed austenitic stainless steel bolted connections," *Eng Struct*, vol. 317, p. 118501, Oct. 2024, doi: 10.1016/J.ENGSTRUCT.2024.118501.

[6] C. Wang, Y. H. Lu, P. Zhu, and T. Shoji, "In-situ observation of deformation behavior of the periodic structure in 316L stainless steel fabricated by wire and arc additive

manufacturing,” *Mater Charact*, vol. 203, p. 113162, Sep. 2023, doi: 10.1016/J.MATCHAR.2023.113162.

[7] V. Ajay, J. Nakrani, N. K. Mishra, and A. Shrivastava, “Fatigue crack growth behavior of SS316L deposition from wire arc additive manufacturing,” *Manuf Lett*, vol. 35, pp. 658–664, Aug. 2023, doi: 10.1016/J.MFGLET.2023.08.060.

[8] W. Liu *et al.*, “A novel wire arc additive manufactured process for 316L stainless steel for pressure vessel applications: Microstructure, mechanical properties and corrosion behaviour,” *International Journal of Pressure Vessels and Piping*, vol. 214, p. 105457, Apr. 2025, doi: 10.1016/J.IJPVP.2025.105457.

[9] M. Vishnukumar, V. Muthupandi, and S. Jerome, “Effect of post-heat treatment on the mechanical and corrosion behaviour of SS316L fabricated by wire arc additive manufacturing,” *Mater Lett*, vol. 307, p. 131015, Jan. 2022, doi: 10.1016/J.MATLET.2021.131015.

[10] X. Duan and X. Yang, “Achieving enhanced strength and ductility in 316L stainless steel via wire arc additive manufacturing using pulsed arc plasma,” *Materials Science and Engineering: A*, vol. 867, p. 144711, Mar. 2023, doi: 10.1016/J.MSEA.2023.144711.